International Journal of Biological, Life and Agricultural Sciences
ISSN: 2415-6612
Vol:13, No:10, 2019

Effect of Copper Ions Doped-Hydroxyapatite 3D Fiber Scaffold

Adil Elrayah, Jie Weng, Esra Suliman

***Abstract*—**The mineral in human bone is not pure stoichiometric calcium phosphate (Ca/P) as it is partially substituted by in organic elements. In this study, the copper ions (Cu^{2+}) substituted hydroxyapatite (CuHA) powder has been synthesized by the co-precipitation method. The CuHA powder has been used to fabricate CuHA fiber scaffolds by sol-gel process and the following sinter process. The resulted CuHA fibers have slightly different microstructure (i.e. porosity) compared to HA fiber scaffold, which is denser. The mechanical properties test was used to evaluate CuHA, and the results showed decreases in both compression strength and hardness tests. Moreover, the *in vitro* used endothelial cells to evaluate the angiogenesis of CuHA. The result illustrated that the viability of endothelial cell on CuHA fiber scaffold surfaces tends to antigenic behavior. The results obtained with CuHA scaffold give this material benefit in biological applications such as antimicrobial, antitumor, antigens, compacts, filling cavities of the tooth and for the deposition of metal implants anti-tumor, anti-cancer, bone filler, and scaffold.

***Keywords*—**Fiber scaffold, copper ions, hydroxyapatite, hardness, *in vitro,* mechanical properties.

I. Introduction

AS the common mineral component of human bones, hydroxyapatite (HA, $Ca_{10}(PO_4)_6(OH)_2$) has been widely used in bone repair [1], as well as biomedical materials [2]-[5], due to its excellent biocompatibility and bioactivity. Because of the flexibility in the structure of apatite, the various ions such as silver, zinc, bismuth, copper, strontium, silicate, and carbonate are substituted in HA structure to improve the properties such as antibacterial property, mechanical strength, and solubility for bone substitutes [6]. Copper ions have reported for enhancing angiogenesis and stimulating endothelial cell proliferation in vitro and in vivo [7]. Moreover, it facilitates the release of vascular endothelial growth factor (VEGF) and cytokines from producing cells [8]. Because of the benefit of copper, doped HA presents an increasing research interest in bone substitutes [9]. It is expected that the incorporation of into HA bioceramics can not only improve their angiogenesis potential but also offer them additional antibacterial property [10]-[15]. Among the available literature, few studies designed copper doped-HA fiber scaffolds and evaluated their mechanic's properties and biological function. In this study, the copper doped-HA fiber scaffold (CuHA) are fabricated by the sol-gel process and the following sintering. The characterization of CuHA fiber scaffold is evaluated by scanning electronic microscopy (SEM). Moreover, mechanical proprieties were tested and evaluated; the further biological response was assessed by used endothelial cells (EC) in vitro.

Jie Weng is with the Key Laboratory of Advanced Technologies of Materials (MOE), School of Materials Science and Engineering, Southwest Jiaotong University, Chengdu 610031, People's Republic of China.

Adil Elrayah is with the Key Laboratory of Advanced Technologies of Materials (MOE), School of Materials Science and Engineering, Southwest Jiaotong University, Chengdu 610031, People's Republic of China (e-mail: adil.karary@yahoo.com).

II. Material and Methods

A. Synthesis of CuHA Powder

All chemicals were purchased from Kelong Chemical (Chengdu, Sichuan, China) and used as received to synthesize $Ca_{9.5}Cu_{0.5}(PO_4)_6(OH)_2$ powders by precipitation method [16]. In brief, 30 ml solution of Na_2PO_4 was added dropwise to 100 ml solution of $[Ca(NO_3)_2{\cdot}4H_2O$ and $Cu(NO_3)_2{\cdot}3H_2O]$ at a rate of 2 ml/min under the stirring. The Cu/(Ca+Cu) was kept to 5% constant total molar concentration. (Cu+Ca)/P molar ratio of the resulted CuHA precipitate was 1.67 in starting reaction solution. At the end of the reaction, the produced solution with white precipitates was heated to 100 ℃ for 5 minutes. After it had cooled to room temperature, the white precipitates were washed with deionized water more time and by ethanol twice. Finally, the product was dried under heat 80 ℃ and grinded to CuHA powder (blue-sky color).

B. Preparation HA and CuHA Fiber Scaffolds

Both HA and CuHA slurry (without calcinations) was prepared using HA and CuHA powders respectively, by adding it into a sodium alginate solution (3 wt. %) at a ratio of 7 to 1 (HA/alginate solution, w/w). Subsequently, the HA and CuHA slurry were placed in a syringe and dispensed in a $CaCl_2$ solution (200 mM) with a cylindrical mold to rapidly solidify the deposit. The fibrous deposit was further pressed down to produce a cylindrical scaffold [17]. Finally, the fibrous structures with (φ 5mm × 10 mm) were sintered at 1200 °C for 44 h [18].

C. Release Ions

To evaluate the influence of ions release from CuHA scaffolds, 0.5 gram of scaffolds, granules were immersed in 10 µL of Phosphate Buffered Saline (PBS) and incubated at 37 °C in a humid atmosphere with 5% CO_2 for 1, 2, 3, and 4 weeks. Cu concentration in the culture medium was measured with SIGMA ALDARICH copper assay kit (Cu, colorimetric method, China) and compared to control (i.e., BM samples) flowing the manufacture's guidelines. Absorbance measurements were performed with a spectrophotometer at 580 & 800 nm. Three samples were used per material (n=3). Meanwhile the CuHA scaffolds particles were collected abs subjected to module analysis to evaluate of possible strength

changes compare with pure HA scaffolds.

D. In vitro Experiment

Human endothelial cells (ECs) were purchased from Sichuan University, and cultured in a medium supplemented with 10% fetal bovine serum (FBS) and 1% penicillin/streptomycin (37 °C, 5% CO_2-95% humidified air). Then, cells were seeded onto HA and CuHA scaffolds at a density of 1×10^5 cells/scaffold and cultured in the same medium. Alamar blue assays determined the proliferation activity of ECs, Alamar blue solution was added and incubated at 37 °C for 4hr. Then, read at 570 - 600 nm with Quant microplate reader (BIO-TEK INSTRUMENT, INC, USA).

III. Results and Discussions

A. X-Ray Diffraction Characterization

The phase components of HA and Cu-doped HA were shown in Fig. 1. It was noted that pure apatite phase (JCPDS 09-0432) had obtained up to 5% in the case of copper substituted hydroxyapatite. When the percentage of ions doped HA, the peak of HA (JCPDS 09-0432) was slightly shifted to diffraction angle at 32.05922◦ and 31.99237, which corresponds to the 2θ values of copper doped-HA and pure HA, respectively.

The XRD result of pure HA and CuHA powders showed peaks at 2 theta = 26◦ and 32◦, respectively, which are assignable to the (002) and (211) planes of HA (PDF# 00-009-432), 2004 respectively. According, the change in 2 theta mentioned previously may refer to the lower ionic radius of copper (0.72Å) compared to calcium (Ca^{2+} (0.99 Å) [2]. The result implied that the copper dopant (with small ionic radius) had slightly influenced the structure of HA powder. Consequently, the final product was composed of the HA phase, and there was no noticeable difference in the copper ions, which may be due to the strong diffraction peak of the HA powder [17].

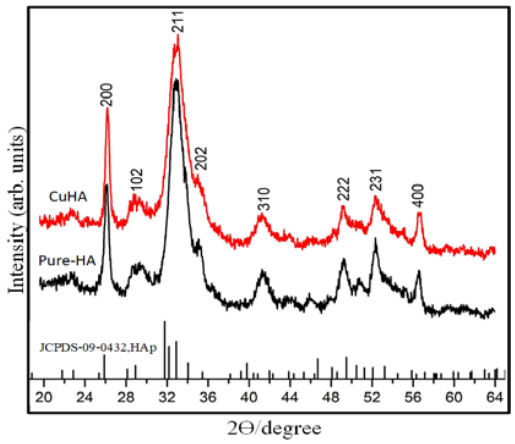

Fig. 1 XRD peaks showed almost the same patterns for pure HA and Cu-doped HA scaffolds

B. Transmission Electron Microscopy (TEM)

Fig. 2 illustrated TEM observations on the HA and CuHA scaffolds. The photomicrographs showed that the size of precipitated HA particles, prepared with and without copper ions. Pure HA powder is constituted of plate-shaped and rod-like crystals, with mean dimensions up to about 50~300 nm, while CuHA powder contains nano-hydroxyapatite rods with the black sphere, with mean dimensions up to about 50~300 nm. The rod-like in CuHA crystallites aggregated into a cluster. Moreover, the presence of copper at the start solution resulted. Also, these results confirmed XRD and FTIR tests.

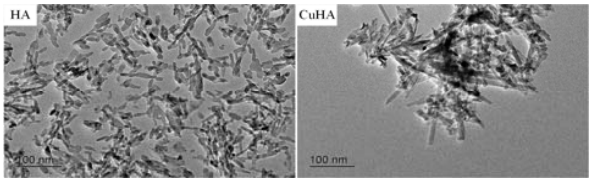

Fig. 2 TEM photograph analysis for HA and CuHA powders

C. FTIR Characterization

The FTIR spectra of all products pure HA powder, CuHA powder, and CuHA scaffold scraped from the sample surfaces showed the characteristic peaks of calcium phosphate (Fig. 3). The peaks at 563 and 598 cm^{-1} were attributed to bending PO_4^{-3}, the peaks at 1038 cm^{-1} to stretching PO_4^{+3}. The absorption peaks at 1374 cm^{-1} broadened for products of CuHA powder and CuHA scaffolds, indicating low crystallinities of the surface deposits [17]. Moreover, the peaks of the products (Pure HA, CuHA powder, and CuHA scaffold) at 1374 and 1458 cm^{-1} were assigned to CO_3^{2+}, which decreased significantly in CuHA scaffolds after sintered. These features suggest that the nanostructured doped synthesized powder in the presence of ions may contain residual and be composed of carbonated apatite with low crystallinities. The FTIR results confirmed the XRD results.

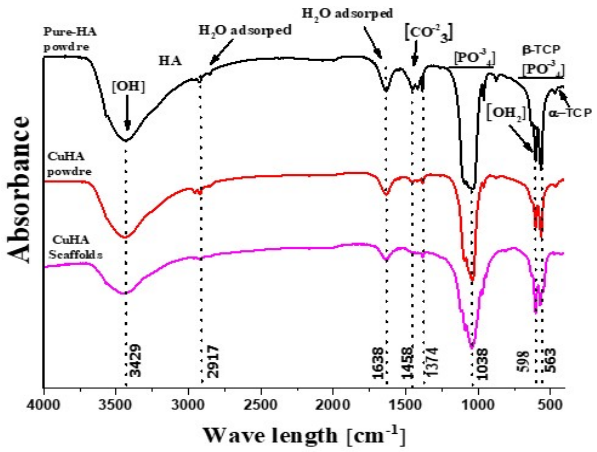

Fig. 3 FTIR spectra characterization showed: HA powder, CuHA powder, and CuHA scaffold peaks

D. Morphological Characterization (SEM)

The HA and CuHA scaffolds morphologies were characterized by Scanning Electron microscopic (SEM), [QUANTA 200) FEI 20 kV] equipped with a dispersive energy X-ray (EDX) spectrometer. All scaffolds were coated with gold

before tested.

The SEM images in Fig. 4 showed the characterization of HA and CuHA scaffolds. Fig. 4 (a) illustrated the morphology of HA fiber scaffolds possessed a porous structure with excellent interconnection. The surface of the CuHA fiber scaffolds was highly porous with a large number of micropores (Fig. 4 (c)), compared with that of HA scaffolds which had less microspore on the surface (Fig. 4 (b)). There is an observable phenomenon happened after the CuHA scaffolds doped and sintered, in which the color of scaffolds was changed from blue-sky before sintered to brown color after 1200 ^{o}C heat treatment.

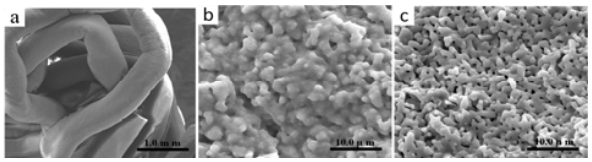

Fig. 4 SEM photographs of HA and CuHA scaffolds (a) the morphology of fibers in scaffolds (b). The HA scaffolds (c) and CuHA scaffolds (D)

E. Release Ions

As mentioned previously, the release rate of copper ions doped-HA can be determined by the dissolution rate of the calcium phosphates and the content of substituted ions [19]. In this study, during 4 weeks immersed in PBS no copper released from CuHA scaffolds. That may occur due to the amount of copper ions which is slightly low. As a result, no copper detected in the digested PBS for 4 weeks.

F. Mechanical Characterization

The compressive mechanical properties of the scaffolds were measured using INSTRON mechanical tester (MTS Systems, Eden Prairie, Minnesota). And the hardness characterization was done with [HXD-1000TM, SHANGHAI]. Scaffolds dimensions are φ 5mm × 10 mm.

For the measurement of compressive strength, HA and CuHA fiber scaffolds have a similar high and width, φ 5 mm x 10 mm. The compressive strength examined against [Load (N)] and [Extend (mm)] of the scaffolds Fig. 5 (A), presented the Bar chart of HA Vs. CuHA scaffolds. The compressive modulus of CuHA scaffolds was done and compared with HA scaffolds. The CuHA scaffolds showed brittle crushing behavior compared with HA scaffolds. That is, owing to its low density resulted from the high porous architecture.

Moreover, the scaffolds tested after 4 weeks PBS immersed. HA and CuHA are reduced in their strength due to the materials degradation during the period. The percentage of loosening strength for each one is about 63%. and 37 % for HA and CuHA respectively. The result implies the CuHA obtained excellent stability after immerged PBS compared to HA scaffolds. That may attribute to copper ions substituted-HA.

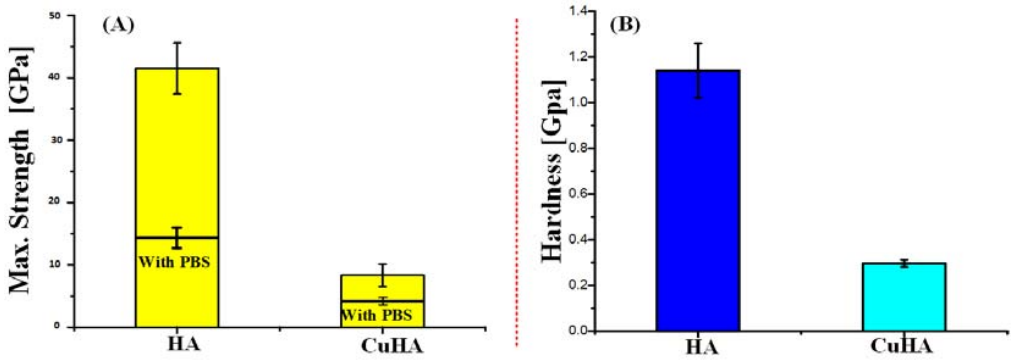

Fig. 5 Mechanical properties test for HA scaffold & CuHA scaffold. (A) The compressive strength examined Bar chart and (B) the hardness Bar graph

Vickers hardness was used to evaluate the hardness on the HA and CuHA scaffolds, as showed in Fig. 5 (B). The hardness test performed for each sample and the average value plotted. The CuHA scaffold showed lower hardness compared to HA. Hence, the lower hardness achieved as a result of low density. The rows and circles in Fig. 6 indicated the typical images after hardness tests completed. The values of hardness for each scaffold are noted as (1.14 and 0.29 GPa) for for HA and CuHA scaffolds respectively. These overall results concluded that the CuHA had decreased the mechanical properties in the compressive strength and hardness test compares with HA scaffolds. But, this result may give the material benefits in biological applications such as filling the tooth and bone.

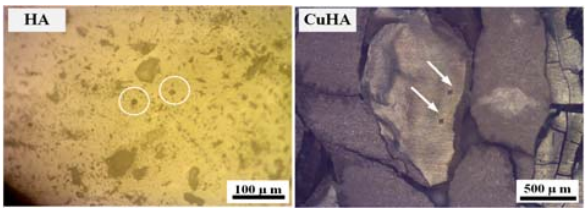

Fig. 6 The hardness tests for HA CuHA scaffolds, the rows and circles demonstrated a typical sign of hardness tests

G. Cell Morphology

In vitro bioactivity was evaluated by immersing the scaffolds in cell culture medium for 7 days. The SEM image in Fig. 7 presented typical morphologies of endothelial cells (ECs) after

7 days culture. SEM Fig. 7 (A) showed the cells appeared well attached over the HA scaffold compared with CuHA scaffold. The ECs morphology on CuHA scaffold looks like slightly loosen the adhesive and connected as shown in Fig. 7 (B). The results presented the ECs morphology on CuHA surfaces which are elongated, oval shaped and they poor connected through cytoplasm extensions as showed. However, the best results obtained in the case of ECs in contact with the HA scaffold. The worst outcome for the test derived from ECs in connection with the CuHA scaffold. Cracks were obtained in the ECs that may have attributed to the fix solutions (alcohol).

The cell culture experimental evaluated the ECs viability and proliferation culture during the time as showed the bar chart (Fig. 8). After 1, 3, 5, and 7 days, the Alamar Blue test showed ECs activities on the HA scaffolds was gradually enhanced while ECs activities on the CuHA scaffolds showed high decreased with a negative correlation. The un-activity of CuHA scaffolds may attribute to the chemical component Cu $(NO_3)_2$, used in the synthesis of CuHA powder as mention previously. Moreover, the component tends towards antibacterial behavior. Kim et al. found that ceramics based on HA made in a wet chemical process with the addition of Cu $(NO_3)_2 \cdot 3H_2O$ had good antimicrobial [20]. But, lower contents of copper dopant are more appropriate for cells, is not cytotoxic [21]. The CuHA scaffolds obtained a lack of a noticeable actively even for the best results which obtained for cells in contact with the scaffold surfaces. Although we suggested the negative influence of CuHA scaffolds is not toxic material but give cells un-activity behavior.

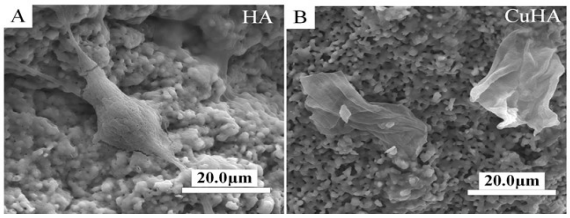

Fig. 7 Endothelial cells after 7 days culture, (A) pure HA, and (B) CuHA scaffolds

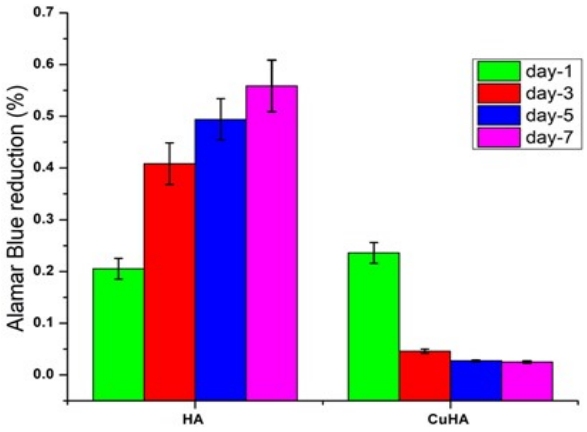

Fig. 8 Column graph presented ECs viability during cell culture descriptive, HA and CuHA scaffolds

IV. Conclusion

Copper ions doped-HA powder were successfully synthesized using precipitation method and fabricated HA and CuHA 3D fiber scaffolds. The HA and CuHA powders were characterized used XRD, TEM, and FTIR. The conclusions from the results are as follows:

1. The presence of copper ions was effected CuHA scaffolds slightly changed the microstructure of scaffolds (i.e., porosity).
2. The presence of copper ions reduced both strength and hardness of CuHA scaffolds.
3. The biological test reported by using in vitro model, gradually decay of the ECs viability on the CuHA scaffolds.
4. The presented results recommend CuHA scaffolds may contribute in future as promising bioceramic material benefit for particular biological applications such as anti-tumor antigens, compacts, scaffold, filling cavities of the tooth and for the deposition of metal implants where the use of metal implants is necessary.

Acknowledgment

This work was supported by the National Key Research and Development Program of China (2016YFB0700803), Karary University Sudan, Khartoum.

References

[1] Elrayah A, Zhi W, Feng S, Et Al. Preparation of Micro/Nano-Structure Copper-Substituted Hydroxyapatite Scaffolds with Improved Angiogenesis Capacity For Bone Regeneration (J). Materials (Basel), 2018, 11(9).

[2] S. Shanmugam And B. Gopal, "Copper Substituted Hydroxyapatite and Fluorapatite: Synthesis, Characterization and Antimicrobial Properties," *Ceramics International,* Vol. 40, Pp. 15655-15662, 2014.

[3] H. R. Bakhsheshi-Rad, E. Hamzah, M. Daroonparvar, M. A. M. Yajid, M. Kasiri-Asgarani, M. R. Abdul-Kadir, *Et Al.*, "In-Vitro Degradation Behavior Of Mg Alloy Coated By Fluorine Doped Hydroxyapatite And Calcium Deficient Hydroxyapatite," *Transactions Of Nonferrous Metals Society of China,* Vol. 24, Pp. 2516-2528, 2014.

[4] A. Farzadi, F. Bakhshi, M. Solati-Hashjin, M. Asadi-Eydivand, And N. A. A. Osman, "Magnesium Incorporated Hydroxyapatite: Synthesis and Structural Properties Characterization," *Ceramics International,* Vol. 40, Pp. 6021-6029, 2014.

[5] S. C. Cox, P. Jamshidi, L. M. Grover, And K. K. Mallick, "Preparation and Characterisation of Nanophase Sr, Mg, and Zn Substituted Hydroxyapatite by Aqueous Precipitation," *Mater Sci Eng C Mater Biol Appl,* Vol. 35, Pp. 106-14, Feb 1 2014.

[6] J. Li, T. Xu, Q. Wang, J. Ren, K. Duan, Y. Mu, *Et Al.*, "Integrating Surface Topography of Stripe Pattern on Pore Surface of 3-Dimensional Hydroxyapatiye Scaffolds," *Materials Letters,* Vol. 169, Pp. 148-152, 4/15/ 2016.

[7] M. A. Saghiri, A. Asatourian, J. Orangi, C. M. Sorenson, And N. Sheibani, "Functional Role of Inorganic Trace Elements in Angiogenesis-Part II: Cr, Si, Zn, Cu, And S," *Crit Rev Oncol Hematol,* Vol. 96, Pp. 143-55, Oct 2015.

[8] R. A. Luca L, Walpoth BH, Gurny R, Jordan O., "The Effects of Carrier Nature And Ph On Rhbmp-2-Induced Ectopic Bone Formation.," *J Control Release* Vol. 147, Pp. 38–44., 2010.

[9] L. Bi, S. Jung, D. Day, K. Neidig, V. Dusevich, D. Eick, *Et Al.*, "Evaluation of Bone Regeneration, Angiogenesis, And Hydroxyapatite Conversion In Critical-Sized Rat Calvarial Defects Implanted With Bioactive Glass Scaffolds," *Journal Of Biomedical Materials Research Part A,* Vol. 100, Pp. 3267-3275, 2012.

[10] Ye J, He J, Wang C, Et Al. Copper-Containing Mesoporous Bioactive Glass Coatings on Orbital Implants For Improving Drug Delivery

Capacity And Antibacterial Activity(J). Biotechnology Letters, 2014, 36(5):961.
[11] M. Othmani, A. Aissa, H. Bachoua, and M. Debbabi, "Surface Modification of Calcium–Copper Hydroxyapatites Using Polyaspartic Acid," *Applied Surface Science,* Vol. 264, Pp. 886-891, 2013.
[12] S. Zhao, H. Wang, Y. Zhang, W. Huang, M. N. Rahaman, Z. Liu, *Et Al.*, "Copper-Doped Borosilicate Bioactive Glass Scaffolds with Improved Angiogenic And Osteogenic Capacity for Repairing Osseous Defects," *Acta Biomater,* Vol. 14, Pp. 185-96, Mar 2015.
[13] C. Stahli, M. James-Bhasin, A. Hoppe, A. R. Boccaccini, And S. N. Nazhat, "Effect of Ion Release from Cu-Doped 45S5 Bioglass(R) On 3D Endothelial Cell Morphogenesis," *Acta Biomater,* Vol. 19, Pp. 15-22, Jun 2015.
[14] H. Wang, S. Zhao, W. Xiao, J. Xue, Y. Shen, J. Zhou, *Et Al.*, "Influence of Cu Doping in Borosilicate Bioactive Glass and the Properties of Its Derived Scaffolds," *Mater Sci Eng C Mater Biol Appl,* Vol. 58, Pp. 194-203, Jan 1 2016.
[15] C. Wu, Y. Zhou, M. Xu, P. Han, L. Chen, J. Chang, *Et Al.*, "Copper-Containing Mesoporous Bioactive Glass Scaffolds with Multifunctional Properties of Angiogenesis Capacity, Osteostimulation And Antibacterial Activity," *Biomaterials,* Vol. 34, Pp. 422-33, Jan 2013.
[16] F. Ren, Y. Leng, R. Xin, And X. Ge, "Synthesis, Characterization and Ab Initio Simulation of Magnesium-Substituted Hydroxyapatite," *Acta Biomater,* Vol. 6, Pp. 2787-96, Jul 2010.
[17] D. Xiao, T. Guo, F. Yang, G. Feng, F. Shi, J. Li, *Et Al.*, "In Situ Formation of Nanostructured Calcium Phosphate Coatings on Porous Hydroxyapatite Scaffolds Using A Hydrothermal Method and the Effect on Mesenchymal Stem Cell Behavior," *Ceramics International,* Vol. 43, Pp. 1588-1596, 2017.
[18] G.-S. Lee, J.-H. Park, U. S. Shin, And H.-W. Kim, "Direct Deposited Porous Scaffolds of Calcium Phosphate Cement with Alginate for Drug Delivery and Bone Tissue Engineering," *Acta Biomaterialia,* Vol. 7, Pp. 3178-3186, 2011.
[19] T. N. Kim, Q. L. Feng, J. O. Kim, J. Wu, H. Wang, G. C. Chen, *Et Al.*, "Antimicrobial Effects Of Metal Ions (Ag+, Cu2+, Zn2+) In Hydroxyapatite," *Journal Of Materials Science: Materials In Medicine,* Vol. 9, Pp. 129-34, 1998.
[20] Ž. Radovanović, B. Jokić, D. Veljović, S. Dimitrijević, V. Kojić, R. Petrović, *Et Al.*, "Antimicrobial Activity And Biocompatibility Of Ag+- And Cu2+-Doped Biphasic Hydroxyapatite/A-Tricalcium Phosphate Obtained From Hydrothermally Synthesized Ag+- And Cu2+-Doped Hydroxyapatite," *Applied Surface Science,* Vol. 307, Pp. 513-519, 2014.
[21] K. Sekine, M. Sakama, And K. Hamada, "Evaluation of Strontium Introduced Apatite Cement as the Injectable Bone Substitute Developments," In *Engineering in Medicine And Biology Society*, 2013, P. 858.